

# Calibrating the Quikscat/SeaWinds Radar for Measuring Rainrate Over the Oceans

David E. Weissman, *Fellow, IEEE*, Mark A. Bourassa, James J. O'Brien, and Jeffrey S. Tongue

**Abstract**—This effort continues a study of the effects of rain, over the oceans, on the signal retrieved by the SeaWinds scatterometer. It is determined that the backscatter radar cross section can be used to estimate the volumetric rain rate, averaged horizontally, across the surface resolution cells of the scatterometer. The dual polarization of the radar has a key role in developing this capability. The relative magnitudes of the radar backscatter depends on the volumetric rain rate, the rain column height and surface wind velocity, the viewing angle, as well as the polarization (due to the oblateness of raindrops at the higher rain rates). The approach to calibrating the SeaWinds normalized radar cross section (NRCS) is to collect National Weather Service Next Generation Weather Radar (NEXRAD) radar-derived rain rate measurements (4-km spatial resolution and 6-min rotating cycles) colocated in space (offshore) and time with scatterometer observations. These calibration functions lead to a Z–R relationship, which is then used at mid-ocean locations to estimate the rain rate in 0.25° or larger resolution cells, which are compared with Tropical Rainfall Measuring Mission (TRMM) Microwave Imager (TMI) rain estimates. Experimental results to date are in general agreement with simplified theoretical models of backscatter from rain, for this frequency, 14 GHz. These comparisons show very good agreement on a cell-by-cell basis with the TMI estimates for both wide areas (1000 km) and smaller area rain events.

**Index Terms**—Next Generation Weather Radar (NEXRAD), precipitation, radar reflectivity, scatterometer normalized radar cross section (NRCS), space-based radar, Tropical Rain Measuring Mission (TRMM).

## I. INTRODUCTION

**R**AIN INTERFERES with the intended application of the measurements of the sea surface's radar cross section by the SeaWinds scatterometer: the estimation of the sea surface wind speed and direction [1], [2]. The presence of rain regions within the boundaries of the illuminated surface area results in additional backscatter from these atmospheric volumes and possibly attenuation of the beam directed toward the surface and the backscatter from the surface [3]. In many cases, depending on the wind magnitude, the backscatter from the rain will augment or dominate the received signal and the measured normalized

radar cross section (NRCS). This results in overestimates of the wind magnitude and meaningless wind direction values [4]. The relatively long duration transmitted pulse provides the equivalent of a continuous-wave radar. The backscatter from the rain volume is the path-integrated value that may include the complete column of rain or possibly a thinner layer when the beam attenuation is large enough to suppress most of the power density before it reaches the sea surface.

The pencil beam geometry of the conically scanning SeaWinds radar is shown in Fig. 1 [2]. The antenna consists of a single 1-m parabolic reflecting dish that accommodates feeds for both vertical and horizontal polarizations. The beams are coplanar and are incident on the surface with angles of 54° and 46°, respectively, from the local zenith. These result in differing radii for the illumination circles on the surface, of about 900 and 700 km. The distance of any wind vector cell (WVC) from the nadir track of the satellite determines the time differential between the V-pol and H-pol  $\sigma_0$  observations. With a spacecraft speed of 7 km/s, the difference in time between the successive illumination of a cell by the V-pol and H-pol beams can be limited to vary only between 29 s (forward look) and 80 s (side look). Relative to the time rates of change of rain structures in the atmosphere and rain rates at the surface, this time differential is viewed as not significant with respect to causing errors in measurements and interpretations within this current study. Collocating measurements with the two different polarizations is straightforward, since each measurement cell is fully documented. When it is desirable to collect pairs of H-pol and V-pol measurements, the distances between the centers of cells for a selected pair are mostly 3–8 km. A separation and grouping was made between those cells viewed by the beams in the “forward” azimuth swing and those viewed in the “aft” azimuth angles. In certain comparisons to be shown below, it was desirable to eliminate the effects of the time difference when a cell is viewed by the forward beam followed by the aft beam, which may be two or more minutes later. This procedure also suppresses some of what would be the azimuth variation of  $\sigma_0$ , when the wind-driven sea surface backscattering is also contributing to the measurement.

Steps were taken to quantify the effect of rain on SeaWinds NRCS, using Next Generation Weather Radar (NEXRAD) Level III rain data for *in situ* measurements, over the ocean and sufficiently far offshore to avoid land contamination issues. The nearly simultaneous NEXRAD composite reflectivity data (“Z” values; e.g., Fig. 2), were converted to rain rate in 4-km cells; then they were combined into an average over an approximate scatterometer footprint (a 28-km<sup>2</sup>), centered at each scatterometer cell. Z is the logarithmic radar reflectivity factor measured in units of decibels relative to a reflectivity of 1 mm<sup>6</sup>/m<sup>3</sup> (dBZ). Each of the colocated SeaWinds NRCSs,

Manuscript received September 19, 2002; revised July 27, 2003. This work was supported in part by the Physical Oceanography Program of the National Aeronautics and Space Administration (NASA) through grants to Hofstra University and the Center for Ocean-Atmospheric Prediction Studies, Florida State University (through support by the NASA OVWST Project, the NASA/OSU SeaWinds Project, and NOPP), and in part by the National Weather Service through a COMET Partners Project grant to Hofstra University administered by the University Corporation for Atmospheric Research, Boulder, CO.

D. E. Weissman is with the Department of Engineering, Hofstra University, Hempstead, NY 11549 USA.

M. A. Bourassa and J. J. O'Brien are with the Center for Ocean-Atmospheric Prediction Studies, The Florida State University, Tallahassee, FL 32306-2840 USA.

J. S. Tongue is with the National Weather Service, Upton, NY 11973 USA.  
Digital Object Identifier 10.1109/TGRS.2003.817975

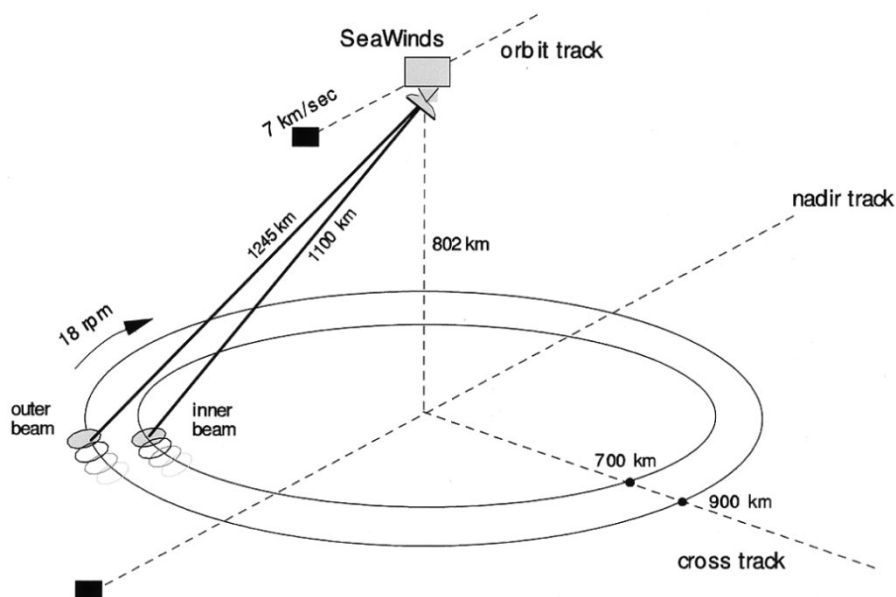


Fig. 1. SeaWinds measurement geometry illustrating the antenna beam locations for the different polarizations. Inner beam is H-pol. Outer beam is V-pol.

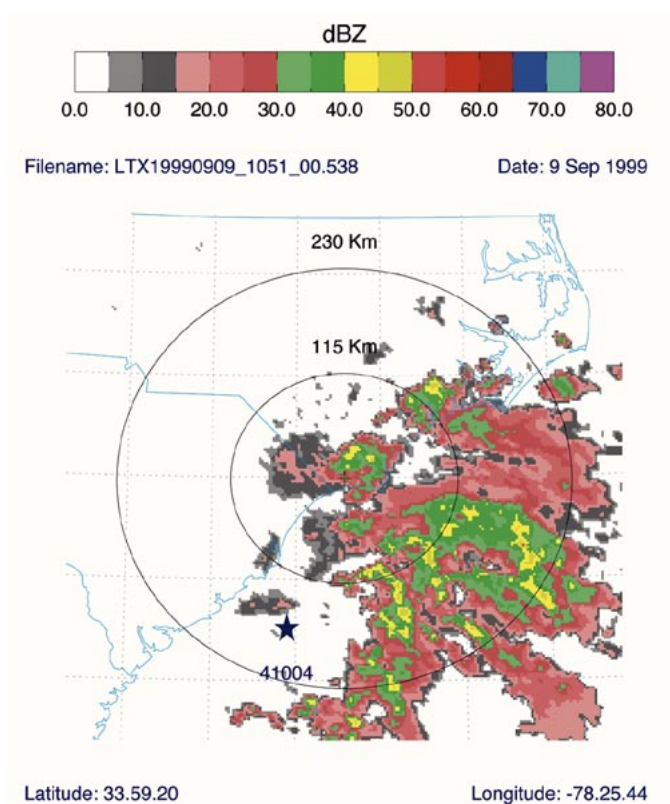


Fig. 2. Composite reflectivity (quantized in 16 discrete dBZ levels) derived from a 6-min scan by the WSR-88D NEXRAD at Wilmington, NC on September 9, 1999. Buoy # 41 004 is indicated by a star symbol.

subset by polarization, are assigned to that average rain rate. The wide variation of the rain intensity within the area spanned by the scatterometer swath results in a sizeable dynamic range of NRCS values. The particular event shown in Fig. 2 was characterized by low winds throughout the region. These data provide the basis of calibration curves for each polarization; these curves are referred to as Z-R functions in radar mete-

orology terminology. These functions are used over the open ocean to convert the Quikscat (QSCAT) L2A NRCS data into rain rate estimates. The rain estimates can then be compared with values derived from the passive Tropical Rainfall Mapping Mission (TRMM) Microwave Imager (TMI) onboard the TRMM satellite. Numerous events in disparate ocean regions were analyzed, and all produced consistently good agreement between the TMI and this SeaWinds-algorithm rain rate for averages over a  $0.5^\circ$  square latitude/longitude region.

## II. BACKGROUND

A key component of the global water cycle is rainfall, which is related to the frequency and intensity of storms. The measurement of rain rate over the global oceans has been a major scientific goal for a long time due to its effect on climate and the biosphere. There are numerous questions, applicable to weather prediction and global climate monitoring, that require more accurate estimates of the water cycle. The Tropical Rainfall Measuring Mission (TRMM) was launched in 1997 to conduct systematic measurements of tropical rainfall. Quoting one of the statements made about the TRMM radar mission, in Kummerow *et al.* [5], “accurate estimates of the amount and distribution of tropical precipitation are desperately needed to validate and gain confidence in large scale models of global warming.” One of the TRMM instruments was a microwave radar [6]. The unique features of this radar, compared to passive techniques, are the ability to penetrate clouds and to use the time resolution of the returning signal to determine vertical profiles the rain rate with high spatial resolution.

Rain is one of the most difficult atmospheric variables to measure due to its heterogeneity (concentration into a few cloud systems), and due to its spatial and rapid temporal variations. Even when sophisticated weather radars perform measurements at a fixed time and location, the estimation of the several rainfall parameters is generally difficult and subject to numerous sources of uncertainty related to the dynamics and the physics of raindrops. Nevertheless, the use of microwave radar for

quantitative precipitation observations has been accepted as the best meteorological method for over 50 years. The development of a QSCAT-related technique will benefit from the large body of knowledge accumulated in the field of radar meteorology for ground-based sensors. Expanding this community of sensors to satellite radars with brief and only periodic observing times at each location advances the spatial coverage, but still leaves significant unmet needs. The SeaWinds radar, with its wide swath, can make a substantial contribution to better spatial and temporal coverage simply because there are no other current spaceborne meteorological radars, besides TRMM. Additional contribution is the advancement of the measurement technique. Limitations of this radar are its large, beam-limited footprint and its lack of frequent temporal sampling. It is too early to determine the limits of precision and coverage that can be achieved with the use of SeaWinds for rain measurements. It is encouraging to note that its 1400-km swath width (for colocated H-pol and V-pol observations), its independence of clouds, and near-real-time observations and data stream provide unique capabilities.

One recent innovation gaining increased application is coherent dual-polarization backscatter measurements to discriminate between the smaller spherical raindrops and the larger oblate drops, the distributions of which are functions of rain rate. The difference of H-pol and V-pol signals due to this effect is called “differential-reflectivity” [7]. While SeaWinds is limited to incoherent dual polarization, it still has the capability to exploit this phenomenon. This differential polarization response of the SeaWinds scatterometer to moderate and large rain rates can be exploited for quantitative precipitation detection and measurement on many different time and spatial scales. This technique has been applied across a wide of frequencies from 3–35 GHz [8]. Of particular relevance to SeaWinds is that Holt [8] shows that the key measurable parameter, the differential reflectivity ( $Z_{DR}$ ), has a very similar dependence on drop size and rain rate at 16 GHz (Ku-band) as it does at 3 GHz (S-Band), which is the nominal National Weather Service NEXRAD radars’ frequency.

We do consider that “bright banding” can affect our  $Z$ – $R$  relationship similar to that of ground-based radars such as the WSR 88D. The data used in this study do contain some bright-banding affects. These are present in the column observed by the polarimetric QSCAT radar where Bergeron precipitation processes occur. These are situations in which raindrops form from ice particles (melting or coalescence). Due to the tropical nature of some of the data used in the study, any bright banding that occurred was at midtropospheric levels where droplet size were small enough to minimize this effect. Applying the  $Z$ – $R$  relationship in higher latitudes must be used with caution as bright-banding effect could result in a significant overestimation of the rain rate. Also, bright-band conditions would not affect the differential reflectivity because of the random orientation of the particles.

### III. APPROACH

The virtually instantaneous collocation of NEXRAD rain measurements with QSCAT and buoy observations is an advance in the quantitative determination of the effect of rainfall on QSCAT NRCS data. The NEXRAD data products

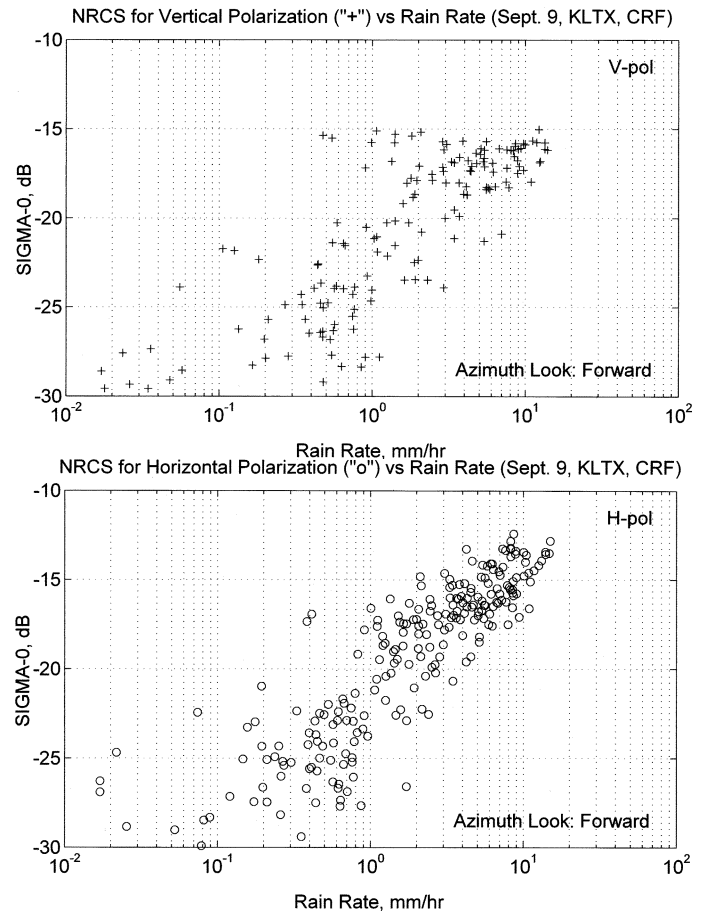


Fig. 3. SeaWinds normalized radar cross-section data (L2A files) versus rain rate. Upper graph is V-pol data. Lower graph is H-pol data. All azimuth look angles are in forward direction. Rain rate is determined from NEXRAD data shown in Fig. 2 (4-km resolution) averaged over 28-km<sup>2</sup> areas centered at each SeaWinds cell. All NRCS data cells used were within 250-km limits from NEXRAD, shown in Fig. 2, and lay within a 150 km × 150 km area. Winds near buoy #41 004 were  $\cong$  3 m/s, and at the eastern edge, at buoy #41002, they were  $\cong$  5.5 m/s.

consist of radar scans taken only 6 min apart, so that the time coincidences with QSCAT observations are sufficiently close to be viewed as effectively instantaneous. Considering how rapidly rain cell spatial structures evolve and how rain intensity varies with time, this close a time difference is essential in order to have a valid observation of the precipitation conditions affecting the QSCAT measurement. The 4-km resolution of NEXRAD is valuable for resolving the spatial variability.

A NEXRAD Level III “Composite Reflectivity” data product with 4-km spatial resolution is shown in Fig. 2. This depicts a maximum S-band reflectivity found on any constant elevation angle azimuthal sweep of a volume scan projected onto each Cartesian grid box [9]. The rain rate is displayed as a quantized color scale for the reflectivity factor ( $Z$ ) in 5-dBZ steps. This example is from the Wilmington, NC station on September 9, 1999. Buoy #41 004 is indicated with a star symbol. The concentric circles are centered at the NEXRAD site (latitude and longitude specified in the figure), and represent range steps of 115 km. The latitude and longitude grid lines are 1° each. Since the QSCAT resolution for a radar cross-section cell is approximated to be 28 km<sup>2</sup>, appreciable averaging of the NEXRAD 4-km resolution elements was necessary to create an equivalent

spatial rain estimate. After converting the NEXRAD RCS from “dBZ” into rain rate and then averaging each  $7 \times 7$  array (equivalent to a  $28\text{-km}^2$  area), a new data array of rain rate, centered at each QSCAT cell location and compatible with the spatial resolution of satellite radar, was produced. The buoy wind measurement, southeast of the rain area (location indicated by a star), had an average of  $1.5\text{ m/s}$  for a 2-h period centered at the time of the QSCAT overpass, with a brief maximum of  $3.2\text{ m/s}$ . Another buoy (# 41 002) on the southeastern side of this rain area (latitude =  $32.3^\circ$ , longitude =  $75.4^\circ$ ) measured winds of about  $5.5\text{ m/s}$  for a 2-h interval around the overpass time. The SeaWinds estimates of wind speeds, in those areas shown where the NEXRAD “rain rate” was  $0\text{ dB}$ , were close to  $5\text{ m/s}$ .

The locations of the QSCAT NRCS points used in this study were constrained to be no farther than  $250\text{ km}$  from the NEXRAD station, over the ocean. Specifically, they lie between  $32^\circ$  and  $34.5^\circ$  latitude and  $-79.5^\circ$  to  $-76^\circ$  longitude. The reason is that the accuracy of near-surface rain estimates decreases with distance from the NEXRAD. The NRCS data points were identified as either horizontal or vertical polarization and separated accordingly. This was straightforward, since they have different incidence angles,  $46^\circ$  and  $54^\circ$ , respectively. Another separation was made which selected NRCS points which were observed by the forward beam sweep of the satellite antenna. This effectively constrains all the data points to be within a narrow range of radar azimuth angles, when the area under study is much less than the  $1400\text{-km}$  swath width. Each data point represents the average NRCS ( $\sigma_o$ ) from an elliptically shaped cell  $25 \times 35\text{ km}$ . The center point of this cell is used as the center of a  $28\text{-km}^2$  area over which the mean rain rate is computed using the  $4\text{-km}$  NEXRAD cells (Fig. 2) formed into  $7 \times 7$  arrays. Fig. 3 shows the separate plots of V-pol and H-pol  $\sigma_o$ 's (converted to decibels) versus the mean rain rates for each corresponding cell. The graphs contain data from those cells which were observed with the forward arc of the rotating antenna beam. This selection was done to avoid the issue of time differences between observations of a cell by both the forward look of the antenna followed a few minutes later by the aft look. Obviously, those NRCS cells which fall in an area without rainfall will not be plotted in this graph. The two datasets span a wide dynamic range: approximately two orders of magnitude. Even though these plots display considerable scatter for both quantities, there is a clear monotonic relationship between NRCS and rain rate. There are basic differences in the two radars that contributes to the data variability. The scatterometer operates effectively in a CW mode and integrates the rain backscatter throughout the full column in the line of sight. The size of the NRCS will depend on the height of the rain column and the rain profile within. The NEXRAD data product, measured in millimeters per hour, is more like a flux quantity representing a flow rate at a specific reference height. In this case, it is the maximum value in a vertical column. Therefore variations in the length of the rain column will affect the NRCS but may not affect the NEXRAD product by the same amount.

At the wind speed regime which is believed to exist at the surface, if no rain were present, the NRCS data points for both polarizations would be in the range from  $-30$  to  $-25\text{ dB}$ . For rain rates larger than  $0.2\text{ mm/h}$ , the NRCS is found to equal or exceed these surface estimates, and both polarization  $\sigma_o$ 's

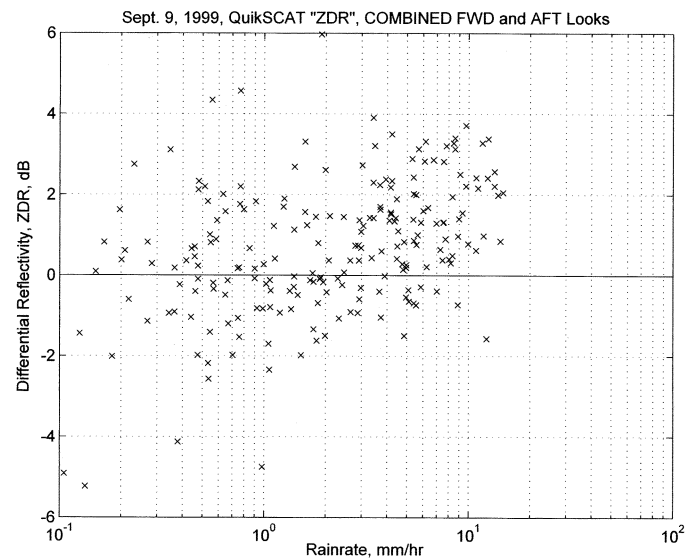


Fig. 4. Differential reflectivity ( $Z_{DR} = \sigma_{oH} - \sigma_{oV}$ ) between collocated scatterometer cells that lie within most of the rain covered area shown in Fig. 2 versus the NEXRAD estimated rain rate in that cell.

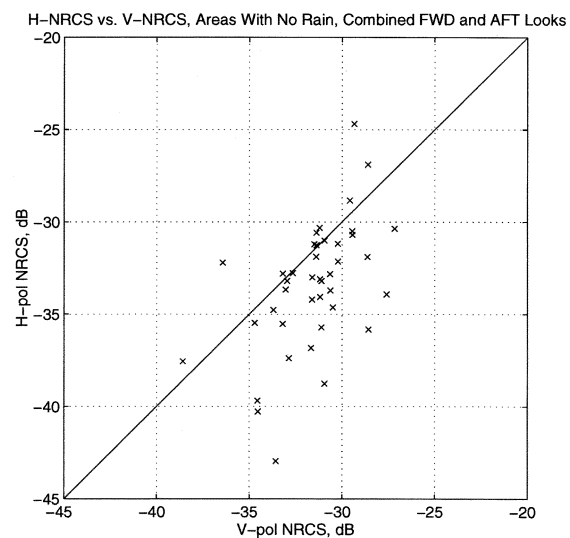


Fig. 5. Comparison between collocated H-pol and V-pol  $\sigma_o$ 's in areas in which the NEXRAD indicates that there is negligible rainfall. This demonstrates that V-pol is generally greater than H-pol due to the nature of sea surface scattering.

clearly increase proportionally to the rain rate. One other issue that will cause scatter in the NRCS data is the variability of the drop size distribution. These uncertainties, while undesirable, do not appear to negate the usefulness of the relationship seen in this figure. Another process that contributes to the NRCS, at the lower wind speeds, is the augmented surface roughness created by the raindrops striking the surface. Detailed measurements of this situation were conducted by Contreras *et al.* [10]. Their measured results, from a ship-based platform, provide a wide range of information. However, further analysis is necessary to interpret them in the context of the satellite radar problem where atmospheric effects are involved. A consideration of the measured  $\sigma_o$ 's in Fig. 3 for rain rates less than  $1\text{ mm/h}$ , at these low wind speeds, suggests that some of the data points above  $-25\text{ dB}$  could be dominated by surface rain-induced roughness.

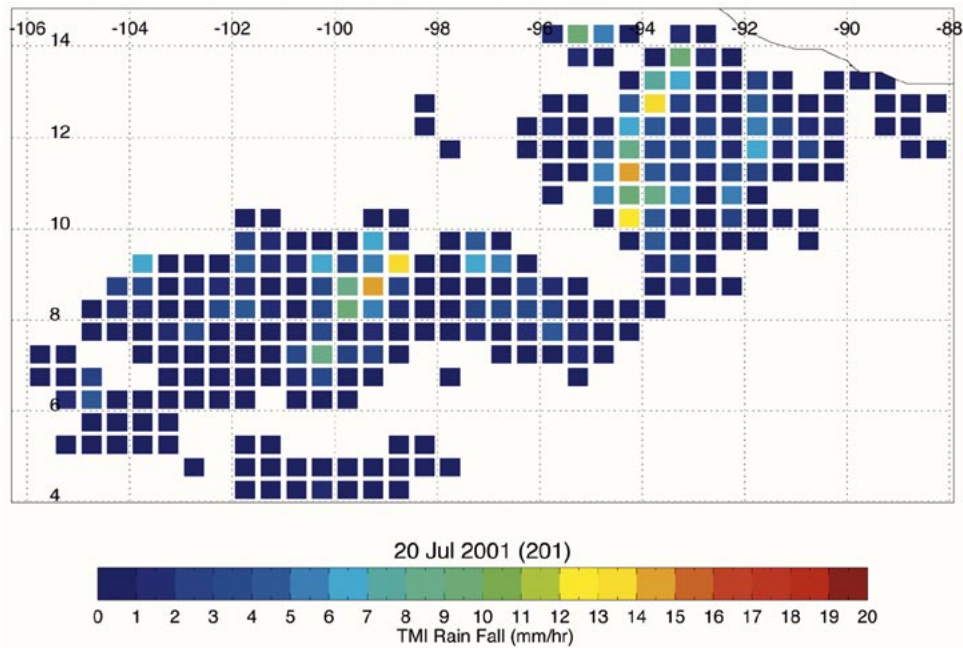


Fig. 6. TRMM-TMI rain rate ( $0.5^\circ$  latitude/longitude bins) measurements over the ocean, west of Nicaragua, on July 20, 2001 at 12:00 GMT, within 5 min of a QSCAT overpass. The color bar indicates rain intensity.

A more careful comparison of the data for rain rates larger than or equal to 1 mm/h (Fig. 3) shows that H-pol NRCS tends to exceed the V-pol. This effect, the differential reflectivity ( $Z_{DR}$ ), is well known in the field of radar meteorology. The physical basis for this is the oblateness of raindrops, once they become larger than about 2 mm in diameter [11]. The lower graph of the H-pol data has been fit with a regression function to create a “Z-R” function for the Ku-band scatterometer. This function is similar to the one developed using a simple theoretical model for spherical raindrops [4]. Comparing one point from Fig. 7 of this reference, the theoretical NRCS for a rain rate of 10 mm/h is  $-16$  dB. Comparing this with the two plots in Fig. 3 here, this value falls between the mean H-pol level of  $-14$  dB, and the mean V-pol measurements of about  $-17$  dB. The H-pol NRCS is proportional to the rain rate, raised to an exponential power of 0.53. This is the empirical function that can then be used to estimate rain rates over the ocean with cell sizes determined by the scatterometer resolution. The  $Z_{DR}$  function is not used as an algorithm to estimate rain rate. It is used to determine that the scatterometer is receiving backscatter from the rain volume. The purpose it serves in this study is as a fairly reliable “rain flag.”

This phenomena is examined more closely by employing the H-pol and V-pol collocation method described in an earlier section. The differential reflectivity  $Z_{DR}$  is computed and plotted (Fig. 4), for pairs of points that satisfy the selection criteria of having cell distances no more than 10 km. The same rain collocation method is also used. The results in Fig. 4 provide definitive evidence that the SeaWinds scatterometer can detect rain of certain magnitudes and may estimate rain rate by applying a relationship based on these results. The two notable features are that for rain rates above 3 mm/h, the majority of  $Z_{DR}$  points exceed zero, and a significant number of these point exceed 2 dB. The latter situation is unexpected, based on studies with ground-based S-band radars and on other theoretical studies.

This larger magnitude cannot be explained with detailed theoretical electromagnetic calculations at Ku-band (using the relevant incident angles) using a recent model for the drop size distribution based on ground-based Ku-band data [12], [13]. This observation is currently under additional study to seek a physical explanation based on all the parameters of this measurement.

A supporting observation can be seen in Fig. 5. Here, a no-rain area was identified in the NEXRAD image (Fig. 2), so that the relative magnitudes of the collocated H-pol and V-pol NRCS could be examined, when the signal returning from the sea surface is only affected by wind. The great majority (80%) of these comparisons indicate that V-pol is greater than or equal to H-pol when rain is not involved. Similar results have been seen in other locations and events. This reinforces the interpretation above that the positive differential reflectivity, in the unique geometry of QScat, is a result of rainfall. This effect can also be useful in the development of “rain flags” that are needed to alert the users of wind vector data products of likely contamination.

#### IV. RESULTS

Several collocations of the TRMM satellite and QSCAT were studied to determine the level of agreement between rain estimates produced by the passive microwave imager (TMI) and the method discussed above. The TRMM product used here, which has a 760-km wide swath, contains daily files with 24 hourly segments of the orbit. The gridded rain rate estimates are in  $0.5^\circ$  cells in units of millimeters per hour and are accompanied by the time of observation. The procedure used here is to survey the rain observations collected by TRMM and then seek a sufficiently close encounter (in space and time) with QSCAT. Numerous events have been studied with similar results.

A good example is an event of July 20, 2001 in an ocean region west of Nicaragua. A section of the hourly segment cor-

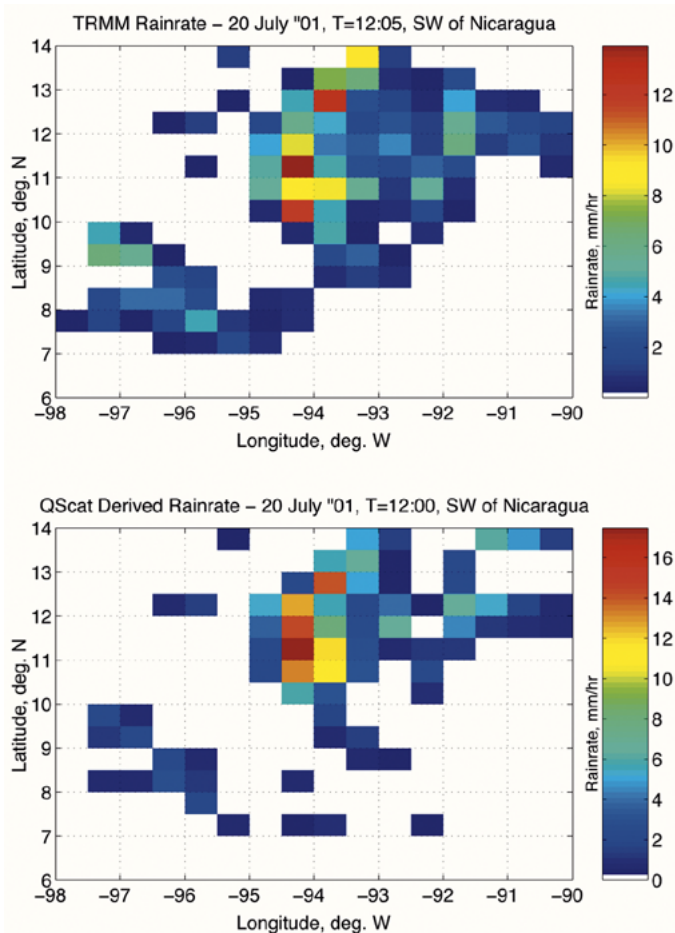


Fig. 7. Comparison between SeaWinds rain rate estimates averaged over  $0.5^\circ$  to match TMI, the data of Fig. 6, which lie within the H-pol swath of the radar. (Upper graph) Subset of the TMI measurements of Fig. 6. (Lower graph) SeaWinds rain rates estimates derived from the H-pol data and an NRCS–Rainrate relationship derived from Fig. 3. The spatial pattern of rain detection by SeaWinds over this ocean region matches TMI very well. Note that the upper and lower colorbars are not identically calibrated.

responding to 12:05Z is extracted from the TRMM data image (Fig. 6). The features here are typical of many other observations. Relative small clusters of high rain rates, often exceeding  $7 \text{ mm/h}$ , occur in areas of  $1^\circ$  to  $2^\circ$  latitude and longitude. These are imbedded in much larger regions of lower rain rates.

A QSCAT orbit collocation was observed at 12:00Z, but with an oblique swath that covered only the region east of  $-99^\circ$  longitude and slanted to exclude some of the section below  $8.5^\circ$  latitude. The higher resolution of the QSCAT L2A data (the highest level dataset containing backscatter observations) are used to estimate mean rain rates in  $0.25^\circ$  cells, using the Z–R relation discussed above. The rain rates are averaged again to create a matching  $0.5^\circ$  cell rain rate. Therefore, a subregion of the rain seen by TMI (Fig. 6) is replotted in Fig. 7 (upper graph) for comparison with the new SeaWinds rain estimates in an identical region in the lower graph. The scatterometer rain rates (lower graph) are seen to provide a very similar spatial image of the rain occurrence and intensity. Some limitations are that the scatterometer may not detect some of the lower rain rates detected by TRMM, but this appears to be minor shortcoming. A point-by-point scatterplot of the TRMM-versus-QSCAT rain rates (Fig. 8) shows those data points where neither has a zero

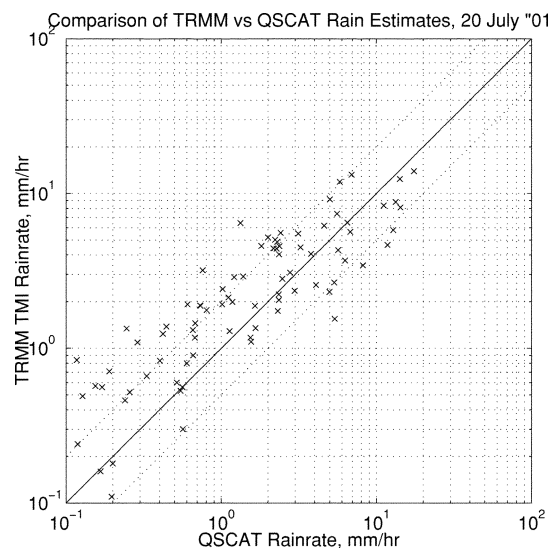


Fig. 8. Point-by-point comparison of TMI rain rates versus SeaWinds rain estimates for cells shown in Fig. 7. The log-log plot was chosen for wide dynamic range. The solid line indicates perfect agreement, with the parallel dashed lines above and below indicating factor-of-two differences. A majority of data point comparisons lie within the dashed lines.

value. The solid line indicates perfect agreement, and the dashed lines show the limits for differences that are less than a factor of two. Clearly, most of the comparison points show that the QSCAT rain estimates are within a factor of two of the TRMM values. A simple summation of all TRMM and QSCAT rain rates over the entire region under study produces very close agreement (within 20%). This consistency will be useful if the two datasets are combined for monitoring precipitation over the global oceans. The general agreement between cell rain rates is better for those rain rates above  $1 \text{ mm/h}$ . Possible reasons for disagreements at the lower rain rates are errors in the TMI at lower rain rates, Qscat errors caused by variations in the height and uniformity of the rain column, and variations in the drop size distribution.

## V. SUMMARY

This study provides evidence on the capability of SeaWinds scatterometer to estimate rain rates over the ocean. The relationships derived from empirical data are consistent with those used in radar meteorology, and applied to weather radar and the Tropical Rainfall Measurement Mission. The principal algorithm was derived from collocated NEXRAD and QSCAT measurements. It also exploits the differential reflectivity associated with moderate and higher rain rates. Analysis is continuing to refine the features and quality of the algorithms for rain flagging as well as rain rate estimation. Our methodology uses a NRCS versus rain rate formula, rather than a Z–R relation. Theoretical studies are in progress to better understand the relative influence of the of the sea surface NRCS at a variety of wind speeds, and drop size distribution parameters [13]. Attention will also be directed at situations with strong wind and storm conditions to test the usefulness and range of validity of this technique. Considering the wide swath of the scatterometer and its global spatial coverage, future applications for global precipitation studies are likely.

## ACKNOWLEDGMENT

The QSCAT Level 2A data were provided by the NASA Jet Propulsion Laboratory PO.DAAC.

## REFERENCES

- [1] F. M. Nader, M. H. Frielich, and D. G. Long, "Spaceborne radar measurement of wind velocity over the ocean—An overview of the NSCAT scatterometer systems," *Proc. IEEE*, vol. 79, pp. 850–866, June 1991.
- [2] M. W. Spencer, C. Wu, and D. G. Long, "Improved resolution backscatter measurements with the SeaWinds pencil-beam scatterometer," *IEEE Trans. Geosci. Remote Sensing*, vol. 38, pp. 89–104, Jan. 2000.
- [3] B. W. Stiles and S. H. Yueh, "Impact of rain on spaceborne Ku-band wind scatterometer data," *IEEE Trans. Geosci. Remote Sensing*, vol. 40, pp. 1973–1983, Sept. 2002.
- [4] D. E. Weissman, M. A. Bourassa, and J. Tongue, "Effects of rain-rate and wind magnitude on SeaWinds scatterometer wind speed errors," *J. Atmos. Oceanic Technol.*, vol. 19, no. 5, pp. 738–746, May 2002.
- [5] C. Kummerow *et al.*, "The status of the Tropical Rainfall Mapping Mission (TRMM) after two years in orbit," *J. Appl. Meteorol.*, pt. I, vol. 39, no. 12, pp. 1965–1982, Dec. 2000.
- [6] R. Meneghini and T. Kozu, *Spaceborne Weather Radar*. Boston, MA: Artech House, 1990.
- [7] R. J. Doviak and D. S. Zrnic, *Doppler Radar and Weather Observations*, 2nd ed. New York: Academic, 1993.
- [8] A. R. Holt, "Some factors affecting the remote sensing of rain by polarization diversity radar in the 3-to-35 GHz frequency range," *Radio Sci.*, vol. 19, no. 5, pp. 1399–1412, 1984.
- [9] G. E. Klazura and D. A. Imy, "A description of the initial set of analysis products available from the NEXRAD WSR-88D system," *Bull. Amer. Meteorol. Soc.*, vol. 74, no. 7, pp. 1293–1311, July 1993.
- [10] R. F. Contreras, W. J. Plant, W. C. Keller, K. Hayes, and J. Nysteuin, "Effects of rain on Ku-band backscatter from the ocean," *J. Geophys. Res.*, vol. 108, no. C5, pp. 34-1–34-13, May 2003.
- [11] V. N. Bringi and V. Chandrasekhar, *Polarimetric Doppler Weather Radar: Principles and Applications*. Cambridge, U.K.: Cambridge Univ. Press, 2001.
- [12] Z. S. Haddad, D. A. Short, S. L. Durden, E. Im, S. Hensley, M. Grable, and R. A. Black, "A new parameterization of the rain drop size distribution," *IEEE Trans. Geosci. Remote Sensing*, vol. 35, pp. 532–539, May 1997.
- [13] S. L. Durden, private communication.



**David E. Weissman** (S'60–M'61–SM'76–F'91) received the B.A. and B.E.E. degrees from New York University (NYU) in 1960, the M.E.E. degree from NYU in 1961, and the Ph.D. degree in electrical engineering from Stanford University, Stanford, CA, in 1968.

From 1963 to 1968, he was a Research Engineer for Stanford Research Institute, Menlo Park, CA. Since 1968, he has been a Faculty Member of the Department of Electrical Engineering at Hofstra University, Hempstead, NY. His research, for over

35 years, has involved the development of microwave radar and radiometric remote sensing techniques for ocean surface observations. These results are published broadly in the engineering and scientific literature. His current research interests enable applications for satellite-based radars (SeaWinds on QuikScat and ADEOS), for the measurement of global ocean wind fields and stress. This includes the study of the effects of rain on scatterometer performance, rain detection, and measurements.

Dr. Weissman was Editor-in-Chief of the IEEE JOURNAL OF OCEANIC ENGINEERING from 1979 to 1982; Conference Technical Committee Co-Chairman for the 1983 IEEE Geoscience and Remote Sensing Society Symposium, and a member of the IEEE Publications board in 1988 and 1989. He has been member of the Administrative Committee of the Oceanic Engineering Society since 1976; Chairman of the Technical Committee on Remote Sensing, OES, since 1985, and is currently Chairman of the OES Fellow Evaluation Committee. Since his election to the Geoscience and Remote Sensing ADCOM in 1999, he has served as Publicity and Public Relations Coordinator and Education Committee Chair. He received a NAS/NRC Senior Postdoctoral Resident Research Associateship at NASA/JPL in 1975. In 1984,

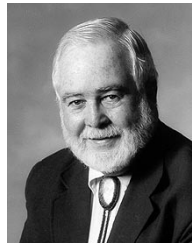
he received the IEEE Centennial Medal (nominated by the Oceanic Engineering Society). In 1977, he received the Best Applications Paper Award for a paper coauthored with James W. Johnson, which was published in the IEEE TRANSACTIONS ON ANTENNAS AND PROPAGATION. In 1995, he was honored with the Oceanic Engineering Society Distinguished Service Award. He received a NASA HQ Citation for Contributions to the NSCAT Scatterometer Project in 1998.



**Mark A. Bourassa** received the B.Sc. degree in physics and the M.Sc. degree in meteorology in 1985 and 1989, respectively, both from the University of Alberta, Edmonton, AB, Canada, and the Ph.D. degree in atmospheric sciences from Purdue University, West Lafayette, IN, in 1993.

He is currently an Assistant Professor in the Department of Meteorology, Florida State University, Tallahassee, and is a member of the Center for Ocean–Atmospheric Prediction Studies. His research interests are air–sea interaction, remote sensing related to air–sea interaction and precipitation, and data fusion.

Dr. Bourassa is a member of the American Geophysical Union and the American Meteorological Society.



**James J. O'Brien** received the B.S. degree in chemistry in 1957, and the M.S. and Ph.D. degrees in meteorology in 1964 and 1966, respectively, all from Texas A&M University, College Station.

He is currently with The Florida State University, Tallahassee, where he is a Robert O. Lawton Distinguished Professor, a Professor of meteorology and oceanography, and Director of the Center for Ocean–Atmospheric Prediction Studies. He also serves as the State Climatologist. He has graduated 36 Ph.D. students and 54 Masters students. He pursues many interests including climatology, physical oceanography, biological oceanography, remote sensing, and numerical modeling of the ocean and the atmosphere.

Dr. O'Brien is a Fellow of the American Association for the Advancement of Science, the American Geophysical Union, the American Meteorological Society, and the Royal Meteorological Society. He is a member of the Oceanographical Society of Japan, SIAM, Chi Epsilon Pi, Phi Kappa Phi, Pi Mu Epsilon, Scarlet Key, and Sigma Xi.

**Jeffrey S. Tongue** received the B.S. degree (with honors) from the State University of New York, College at Oneonta, Oneonta, in 1981, and the M.S. degree from Texas A&M University, College Station, in 1987, both in meteorology.

He is currently the Science and Operations Officer for the National Oceanic and Atmospheric Administration's National Weather Service Forecast Office, Upton, NY. He is also an Associate Professor of earth and space science at Suffolk County Community College, Selden, NY, as well as a U.S. Air Force Reserve Weather Officer. His research interests include remote sensing and data assimilation for operational weather forecasting.

Mr. Tongue is a member of the American Meteorological Society and the National Weather Association.